

Developments in Understanding the Formation, Structure and Properties of Polymer Networks

R.F.T. Stepto,¹ J.I. Cail,¹ D.J.R. Taylor,¹ I.M. Ward,² R.A. Jones²

¹Polymer Science and Technology Group, Manchester Materials Science Centre, UMIST and University of Manchester, Grosvenor Street, Manchester, M1 7HS, UK
E-mail: rfts@tesco.net, j.i.cail@tesco.net

²IRC in Polymer Science and Technology, Department of Physics, University of Leeds, Leeds, LS2 9JT, UK

Summary: Two areas of networks modelling are described. The first is concerned with the application of a Monte-Carlo (MC) algorithm to account fully for loop formation in $RA_2 + R'B_3$ and $RA_2 + R'B_4$ polymerisations. The resulting interpretation of experimental elastic moduli of HDI-based polyurethane (PU) networks prepared at different dilutions shows it is essential to account for elastic losses in loop structures of all sizes. An important parameter, x , is introduced, namely the average fractional loss of elasticity per larger loop structure relative to the loss per smallest loop structure. Application of the MC calculations to the formation and resulting structures of MDI-based PU networks and poly(dimethyl siloxane) (PDMS) networks shows the competing effects of loop structures and chain interactions (PU) or topological entanglements (PDMS) on the modulus. The second area of networks modelling is the MC simulation of the elastic behaviour of chains in networks using realistic rotational-isomeric-state chain models. Stress-strain and stress-optical properties can be modelled quantitatively. In stress-strain behaviour, an increase in the proportion of fully extended chains with increasing macroscopic strain causes a reduction in network modulus at moderate macroscopic strains. There is no need to invoke a transition from affine to phantom chain behaviour as deformation increases. For stress-optical properties, the MC method gives, in agreement with experiment, values of stress-optical coefficient that are dependent upon both deformation ratio and network-chain length. Applications of the method to the quantitative modelling of the stress-strain properties of PDMS networks and the stress-optical properties of polyethylene and poly(ethylene terephthalate) networks are described.

Keywords: modeling; networks

Introduction

This paper describes the results from two aspects of fundamental network studies, namely, modelling the absolute value of modulus from reactant structures and formation conditions, and modelling stress-strain and stress-optical properties.

Absolute Value of Modulus: Relationships between concentrations of chains and junction points that assume perfect network structures are often used when interpreting elastic properties of endlinked networks^[1]. The assumption is rarely true and deviations from perfect

network structures may be due to chain topological entanglements and interactions, to side reactions, incomplete reaction in endlinking polymerisations (giving loose ends) and, more fundamentally and generally, inelastic chain or loop formation from the intramolecular reaction of pairs of groups. Hence, to understand and predict elastomeric properties, it is important to be able to model, statistically, the molecular growth leading to network formation. Further, by considering polymerisations at various dilutions of reactive groups, it is possible to evaluate the effects of loop formation resulting from intramolecular reaction.

Stress-Strain and Stress-Optical Behaviour: Calculations of elastomeric properties of polymer networks have conventionally used theories and models based on the behaviour of a collection of “average” chains, with all the chains responding identically to external forces^[2-4]. Although the molecular origin of the elastic force in a rubber-like material has long been acknowledged, the relationships between deformations at the macroscopic and molecular levels are not yet fully understood. It is thought that the initial network-chain deformation accompanying sample deformations is affine in the macroscopic strain, giving rise to the experimentally observed initial network modulus; as the macroscopic deformation increases, the modulus is seen to decrease because the network chain deformation deviates from affine. A Monte-Carlo (MC) approach developed by the authors^[5,6] has shown that the different responses of individual chains have to be accounted for in defining overall, statistical-mechanically averaged network behaviour and properties. Actual, rather than equivalent Gaussian or Langevin, network-chain end-to-end distance distributions are used. This paper summarises the approach and its applications to stress-strain and stress-optical behaviour.

Absolute Value of Modulus

Monte-Carlo Polymerisation Algorithm

Detailed characterisation of the connectivity, or topology, of networks by experimental means is impossible. In order to investigate the effects of network connectivity on elastomeric properties one must use numerical simulations of the network-forming nonlinear polymerisations. In such simulations, it is important to account for the occurrence of loop-structures of various sizes resulting from intramolecular reaction, with their probabilities of formation correctly weighted. To this end, a MC nonlinear polymerisation algorithm has been developed^[7-9] to simulate self-polymerisations (RA_f), and two-monomer polymerisations of

the general type $RA_{fa} + R'B_{fb}$. All the connections are recorded as a function of extent of reaction of A- or B-groups, and sol fraction, gel fraction and average degrees of polymerisation are calculated. Ring-size distributions have been evaluated and have been found to be very broad.

Correlation of Model Network Topologies with Measured Network Moduli

For a trifunctional network, each smallest loop structure renders three chains inelastic and larger loops are subject only to partial losses in elasticity. These considerations lead to the expression for the modulus, relative to that of the perfect network structure,

$$G^o / G = M_c / M_c^o = 1 / (1 - 6p_{re,1} - x \cdot 6p_{re,i>1}), \quad (1)$$

where G^o is the modulus of the (unswollen) perfect network, G is that of the actual network, M_c is the (number) average molar mass of elastically active chains connecting pairs of junction points in the actual network and M_c^o is that in the perfect network. $p_{re,1}$ is the extent of reaction at complete reaction leading to smallest loops, and $p_{re,i>1}$ is the extent of reaction at complete reaction leading to larger loops. x is the fractional loss of elasticity for chains in loop structures larger than the smallest. Tetrafunctional network structures lose only 2 elastic chains per smallest loop and in this case

$$G^o / G = M_c / M_c^o = 1 / (1 - 4p_{re,1} - x \cdot 4p_{re,i>1}). \quad (2)$$

$p_{re,1}$ and $p_{re,i>1}$ are predicted using the MC nonlinear polymerisation algorithm.

HDI-Based Polyurethane Networks

In the absence of theoretical evaluations of entropy reductions in loop structures, estimates of x can be made using experimentally determined values of M_c / M_c^o . This has been done for polyurethane (PU) networks based on hexamethylene diisocyanate (HDI) reacting with polyoxypropylene (POP) triols and tetrols. The results, for six series of networks prepared in bulk and at various dilutions in solvent, are shown in Fig. 1. The theoretical curves have been fitted^[7-9] by choosing least-squares values of a ring forming-parameter, λ_{a0} , and x . In this respect, it should be noted that $p_{re,1}$ and $p_{re,i>1}$ depend on λ_{a0} , the functionality, f , and the initial ratio of the reactive A- and B-groups.

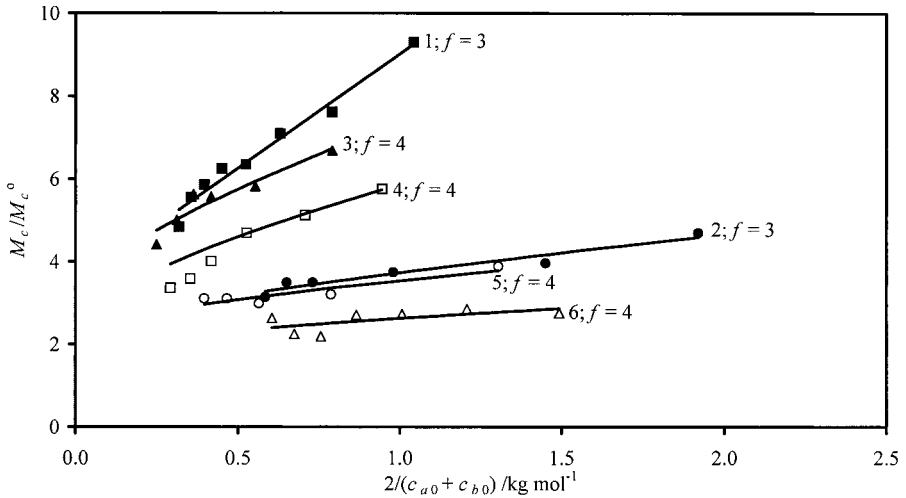


Figure 1: Experimental and calculated values of M_c / M_c^o at complete reaction as functions of the average initial dilution of reactive groups, $2/(c_{a0} + c_{b0})$, for six series of PU networks from stoichiometric reaction mixtures. 1,2: trifunctional networks from polyoxpropylene (POP) triols of different molar masses and hexamethylene diisocyanate (HDI). 3-6: tetrafunctional networks from POP tetrols and HDI. For details of the parameters used to fit the experimental values of M_c / M_c^o , see reference 8.

MDI-Based PU Networks and PDMS Networks

Experimental results of Stanford and Stepto and Ilavsky and Dušek on diphenyl methane diisocyanate (MDI)-based PU networks and of Llorente and Mark on trifunctional and tetrafunctional poly(dimethyl siloxane) (PDMS) networks have been subjected^[10,11] to the same analysis using the MC nonlinear polymerisation algorithm. In contrast to the HDI-based PU networks, the enhancement of modulus by chain interactions (incipient segmentation) and chain entanglements are apparent, respectively, in the MDI-based PU networks and the PDMS networks. Interestingly, the analysis shows that in the MDI-based PU networks (based on the same triol as that used in system 1 in Fig. 1) about 80% of the network chains are associated and the resulting enhancements in modulus for networks prepared at different initial dilutions more or less exactly counteract the decreases due to loops, to give moduli just less than that of the perfect network. On the other hand, the PDMS networks are found to have on average about 1.7 entanglements per chain that counteract the effects of loops to give resulting moduli that are between 10% and 30% greater than those expected for the perfect networks.

Stress-Strain Behaviour^[5,6]

The first stage in this MC simulation involves the numerical generation of the radial end-to-end distance distribution, $W(r)$, for unperturbed chains of various numbers of skeletal bonds (n) at a given temperature according to a rotational-isometric-state (RIS) or other realistic model that reproduces known individual chain dimensions and properties. The corresponding values of probability density $P(r)$, are evaluated as $W(r)/4\pi r^2$, assuming the random orientation of chains in three dimensions.

The second stage concerns simulation of the elastic behaviour of a network. The “network” is represented by a sample of spherically-symmetrical individual chains in a Cartesian laboratory-reference frame; one end of each chain is fixed at the origin. The chains are deformed uniaxially by a deformation ratio, λ , with $\lambda_x \lambda_y \lambda_z = 1$ (i.e. constancy of volume). The end-to-end distances are allowed to increase only up to their effective, conformational maximum, r_{max}^* , above which $W(r) = 0$ according to the sampled $W(r)$. For an individual polymer chain, in a network of N chains, the Helmholtz energy change upon deformation at an absolute temperature T , is assumed to arise solely from the corresponding entropic change. Hence,

$$\Delta A / NkT = \ln\{P(\mathbf{r}_o) / P(\mathbf{r}_{def})\} \quad , \quad (3)$$

where the subscripts “o” and “def” denote the relaxed and deformed end-to-end vectors, respectively.

In the MC scheme, a chain of end-to-end distance r_o , is first chosen, in proportion to $W(r_o)$. The X - and Y - coordinates of its “free” chain-end are chosen randomly, and the Z -component defined consistent with \mathbf{r}_o . Uniaxial deformations, using a series of values of λ are applied in the Z -direction (i.e. $\lambda = \lambda_z$) and the deformed end-to-end distances calculated by simple geometry, with $\lambda_x = \lambda_y = 1/\sqrt{\lambda}$. Any values of r_{def} in excess of r_{max}^* are put equal to r_{max}^* , thus limiting r to the range of values determined by the bond-conformational energies and consistent with $W(r)$. The associated value of $W(r_{def})$ is ascertained, and $\ln P(\mathbf{r}_{def})$ evaluated. The Helmholtz energy change is evaluated via equation (3), and the average change per chain at each λ calculated as

$$\Delta A / NkT = \frac{1}{N} \sum_{i=1}^N \ln \{ P(\mathbf{r}_o) / P(\mathbf{r}_{def}) \} \quad , \quad (4)$$

where N is the number of chains in the M-C sample. Typically, $N = 5 \times 10^6$. The network Helmholtz energy change can be expressed as a function of λ with

$$\Delta A / NkT = s(\lambda^2 + 2/\lambda - 3) \quad (5)$$

For so-called Gaussian networks with affine chain deformation, a plot of $\Delta A/NkT$ versus $\lambda^2 + 2/\lambda - 3$ is linear, with $s = 1/2$. In general, s will be a function of λ and the corresponding normalised stress per unit *unstrained* cross-sectional area is

$$\frac{\sigma}{RT\rho} = \frac{1}{M_c} \left\{ 2s(\lambda - 1/\lambda^2) + (\lambda^2 + 2/\lambda - 3) \frac{ds}{d\lambda} \right\} . \quad (6)$$

The values of s and $(\lambda^2 + 2/\lambda - 3)ds/d\lambda$ effectively describe the deviation of the simulated elastic behaviour from that of a bulk Gaussian network (with the same M_c), for which $s = 1/2$, $ds/d\lambda = 0$ and $\sigma = (\rho RT/M_c)(\lambda - 1/\lambda^2)$. Values of $\sigma/RT\rho$ may be converted to normalised reduced stress, $[\sigma^*]/RT\rho$, where

$$[\sigma^*] = \frac{\sigma}{\lambda - 1/\lambda^2} . \quad (7)$$

Conventionally, the effects of non-Gaussian, non-affine behaviour are represented as positive slopes of the so-called Mooney-Rivlin plots, $[\sigma^*]$ versus $1/\lambda$.

Correlation with Experimental Data on PDMS Networks

The simulated PDMS-network stress-strain data are compared in Fig. 2 with the experimental results of Erman and Flory^[13]. Simulated values of $[\sigma^*]$ were equated with experimental values of $[\sigma^*]/\phi_2^{1/3}$ at a reciprocal extension of $1/\lambda = 0.9$, to define an effective MC chain length, n_{M-C} , for each set of experimental results, equivalent to choosing the value of the initial modulus or M_c . Having thus established n_{M-C} , the simulated Mooney-Rivlin curve can be determined from the variation of $[\sigma^*]/RT\rho$ with $1/\lambda$ for that value of n_{M-C} . The results in Figs. 2(a) and 2(b) show that the simulated stress-strain behaviour provides a satisfactory representation of the experimental data. It is not necessary to invoke a transition from affine to phantom chain-behaviour as strain increases.

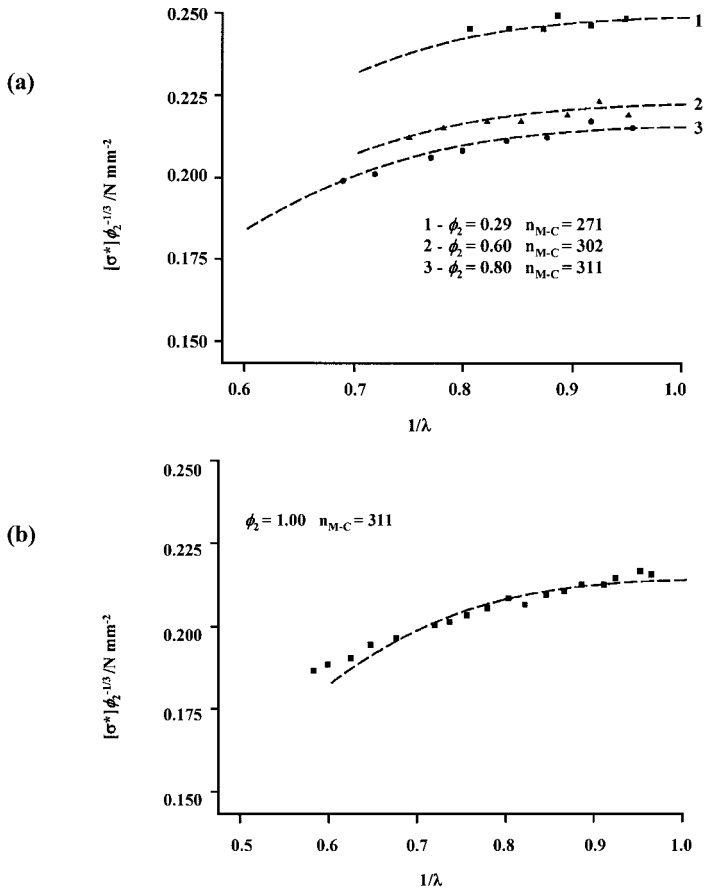


Figure 2: MC Mooney-Rivlin curves fitted^[5] to experimental data^[13]; (a) networks swollen in dodecane, (b) dry network. $T = 293\text{K}$, density of dry network = 974 kg m^{-3} . ϕ_2 = network volume fraction; n_{M-C} = number of bonds in MC chains required to fit $[\sigma^*]/RT\rho$ at $1/\lambda \approx 0.9$.

Stress-Optical Behaviour: Segmental Orientation and Chain Extension

The example of polyethylene (PE)^[14,15] is mainly considered here. The work is presently being extended to poly(ethylene terephthalate) (PET)^[16]. The first stage of the modelling procedure involves the calculation of the average segment angle, ξ , relative to the chain end-to-end vector (\mathbf{r}), for individual chains as a function of chain extension. The orientation function, $\langle P_2(\xi) \rangle = \frac{1}{2}(3\langle \cos^2 \xi \rangle - 1)$, averaged over all the segments in a MC sample is evaluated as a function of r/r_{max} for chains of given numbers of skeletal bonds, n .

The network is subsequently represented by an array of individual chains, initially randomly oriented in three dimensions. It is deformed uniaxially as in the stress-strain simulations of the previous section. The resulting changes in $\langle P_2(\xi) \rangle$, the associated changes in the angle between the end-to-end vector and the uniaxial strain direction, ψ , and, hence, the orientation function, $P_2(\psi)$, are calculated. From these quantities, the average bond orientation, $\langle P_2(\zeta) \rangle$, over all chains, i , in the MC sample, relative to the uniaxial strain direction, is calculated using the Legendre addition theorem, with

$$\langle P_2(\zeta) \rangle = \langle \langle P_2(\xi) \rangle_i \cdot P_2(\psi_i) \rangle . \quad (8)$$

MC Simulation of Network Stress-Orientation Behaviour

The stress-strain behaviour is analysed according to equation (6), recast to give the normalised, true stress, $t/RT\rho$,

$$\frac{t}{RT\rho} = \frac{1}{nM_o} \left\{ 2s(\lambda^2 - \frac{1}{\lambda}) + (\lambda^3 - 3\lambda + 2) \frac{ds}{d\lambda} \right\} . \quad (9)$$

M_o is the average molar mass per skeletal bond, such that $M_c = nM_o$. For the MC sample of chains, the values of t and $\langle P_2(\zeta) \rangle$, evaluated according to equations (8) and (9) are determined as functions of λ . Significantly, it is found that $\langle P_2(\zeta) \rangle$ is not a linear function of the t ; a behaviour that is different from that predicted by the Gaussian, Kuhn and Gr \ddot{u} n model.

To correlate with experimental data, the stress-orientational coefficient, Z_t , is defined, namely,

$$Z_t = \left[\frac{\langle P_2(\zeta) \rangle \rho RT}{t} \right]_{\lambda \rightarrow 1} . \quad (10)$$

The nonlinear behaviour of $\langle P_2(\zeta) \rangle$ with respect to t means that Z_t is not a constant, independent of t or λ . Correction of experimental values of Z_t to values for $\lambda \approx 1$, or $t \approx 0$, gives excellent agreement with experiment, as shown in Fig. 3. The experimental values of Z_t have been calculated using the equation

$$Z_t = \frac{C_{\text{expt}} \rho RT}{1.77 \Delta \tilde{n}_{\text{max}}} , \quad (11)$$

where $\Delta \tilde{n}_{\text{max}}$ is the maximum possible birefringence, corresponding to all segments aligned with the direction of strain, C_{expt} is the measured value of the stress-optical coefficient (at $\lambda = 1.1$ to 1.2) and 1.77 is the correction factor needed to reduce C_{expt} to the value

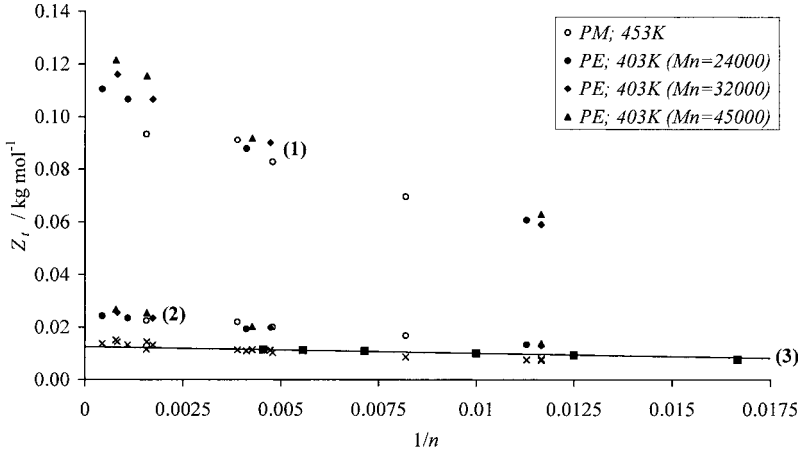


Figure 3: Z_t versus $1/n$ calculated for model networks of 40-bond to 220-bond PE chains (■), compared with values of Z_t derived from Saunders' experimental values of the stress-optical coefficient assuming Z_t is a constant with (1) $\Delta\tilde{n}_{max} = 0.049$ (Bunn and Daubeny) and (2) $\Delta\tilde{n}_{max} = 0.223$ (Denbigh), and (3) equation (11) with $1.77 \times \Delta\tilde{n}_{max} = 1.77 \times 0.223 = 0.395$ (x).

expected as $\lambda \rightarrow 1$. Agreement between experiment and theory is achieved using a value of $\Delta\tilde{n}_{max}$ of 0.223, calculated using Denbigh's polarisabilities based on data for gaseous CH_4 and C_2H_6 . (The value of $\Delta\tilde{n}_{max}$ of 0.223 may be compared with a value of 0.049 calculated on the basis of Bunn and Daubeny's experimental measurements of paraffin crystals. The results obtained for Z_t using $\Delta\tilde{n}_{max} = 0.049$ are also shown in Fig. 3.)

The extension of the detailed modelling of stress-orientational behaviour to PET has used data on melts, where the networks are composed of entangled chains. Preliminary theoretical results^[16] show that, because of the distribution of lengths of entangled chains, the stress-strain behaviour is characterised by an average chain-length longer than that characterising the stress-optical behaviour.

Conclusions

Absolute Value of Modulus: The simulation results shows the importance of accounting fully for loop formation when interpreting the absolute values of the moduli of networks. Even for reactants of high molar mass, the effects of loops on elastic modulus are significant. Model networks are *not* perfect networks and the effects of loops have to be considered,

alongside those of loose ends and chain interactions and entanglements, when interpreting modulus. For PU networks based on HDI and POP polyols, the effects of loops are dominant. For PU networks based on MDI and POP polyols, the effects of loops are present but are counteracted by increases in modulus due to chain interactions. For PDMS networks, using a linear reactant of molar mass greater than the entanglement molar mass, the reductions in modulus due to loops are significant, but are outweighed by those due to entanglements.

Stress-Strain and Stress-Optical Behaviour: The described M-C network simulations, using chains limited to their natural, conformational full extension, are able to reproduce experimentally-observed deviations from affine, Gaussian network-chain behaviour at moderate uniaxial deformations. The concepts of a phantom chain-behaviour and junction-point fluctuations are not required. Decreases in the rate of Helmholtz energy change with deformation of the network occurs naturally as an increasing proportion of network chains becomes fully-extended.

The detailed MC modelling of stress-optical behaviour has provided the quantitative interpretation of the measured stress-optical coefficient of PE, resolving a long-standing discrepancy between theory and experiment. With respect to both PE and PET, there are also important technological implications arising from the realistic analyses carried out. For example, tensile-drawing behaviour, used in the production of fibres and films, is often understood in terms of the stretching of a molecular network, whose junction points are formed by molecular entanglements. Because of the MC modelling, calculation of the maximum draw ratio achievable and, hence, the enhancement of physical properties such as modulus and strength, can now be more accurately related to measured stress-optical properties.

Acknowledgements

Support of the EPSRC and Accelrys for provision of their Polymer Software is gratefully acknowledged.

1. R.F.T. Stepto, in *Polymer Networks – Principles of Their Formation, Structure and Properties*, ed. R.F.T. Stepto, Blackie Academic & Professional, London 1998, Chapter 2
2. L.R.G. Treloar, *The Physics of Rubber Elasticity*, 3rd ed., Oxford University Press, Oxford 1975
3. P.J. Flory, *Proc. Roy. Soc. London, Ser. A* **351**, 351 (1976)
4. J.E. Mark and B. Erman, in: *Polymer Networks – Principles of their Formation Structure and Properties*, ed. R.F.T. Stepto, Blackie Academic & Professional, London 1998, Chapter 7
5. R.F.T. Stepto and D.J.R. Taylor, *Macromol. Symp.* **93**, 261 (1995)
6. R.F.T. Stepto and D.J.R. Taylor, *J. Chem. Soc., Faraday Trans.* **91**, 2639 (1995)
7. S. Dutton, R.F.T. Stepto and D.J.R. Taylor, *Angew. Makromol. Chem.* **240**, 39 (1996)
8. R.F.T. Stepto and D.J.R. Taylor, in *Cyclic Polymers*, 2nd edition, ed. J.A. Semlyen, Kluwer Academic Publishers, Dordrecht 2000, Chapter 15
9. R.F.T. Stepto, J.I. Cail and D.J.R. Taylor, *Polimery* **XLV**, 455 (2000)
10. R.F.T. Stepto, J.I. Cail and D.J.R. Taylor, *Mat. Innovation* **in press**
11. R.F.T. Stepto, J.I. Cail and D.J.R. Taylor, *Polymer Prepr.* **42**(1), 117 (2000)
12. J.I. Cail, R.F.T. Stepto, D.J.R. Taylor, R.A. Jones and I.M. Ward, *Physical Chem. Chemical Phys.* **2**, 4361 (2000)
13. B. Erman and P.J. Flory, *Macromolecules* **16**, 1607 (1983)
14. D.J.R. Taylor, R.F.T. Stepto, R.A. Jones and I.M. Ward, *Macromolecules* **32**, 1978 (1999)
15. J.I. Cail, D.J.R. Taylor, R.F.T. Stepto, M.G. Brereton, R.A. Jones, M.E. Ries and I.M. Ward, *Macromolecules* **33**, 4966 (2000)
16. I.M. Ward, M. Bleackley, D.J.R. Taylor, J.I. Cail, and R.F.T. Stepto, *Polym. Engg. Sci.* **39**, 2235 (1999)